Preparation and Properties of a Rigid Hemp Shiv Insulation Particle Board Using Citric Acid-Glycerol Mixture as an Eco-Friendly Binder

Simon Pepin,[a,*] Mike Lawrence,[b,c] and Pierre Blanchet [a]

*Corresponding author: simon.pepin.1@ulaval.ca

DOI: 10.15376/biores.19.4.9310-9333

GRAPHICAL ABSTRACT

Preparation and Properties of a Rigid Hemp Shiv Insulation Particle Board Using Citric Acid-Glycerol Mixture as an Eco-Friendly Binder

Simon Pepin,[a,*] Mike Lawrence,[b,c] and Pierre Blanchet [a]

Particle boards are commonly manufactured from wood-based material bound with a thermosetting adhesive based on the reaction of formaldehyde with phenol, urea, melamine, or co-condensates. The use of formaldehyde is a cause for concern due to its harmful emissions. This study investigates the use of an alternative binder combined with particles derived from a short-cycle crop as an alternative to timber derived particles. A low density particle board was developed using hemp shiv as an aggregate with a binder made with crude glycerol, derived from the waste stream of the bio-diesel industry, esterified with citric acid under heat activation. This board was characterized and found to have good mechanical properties, low thermal conductivity, and good moisture buffering. Dimensional stability was compromised by swelling when exposed to water, but it will be possible to address this shortcoming using hydrophobic additives. The acoustic properties of the board were also found to be excellent, showing potential for use as a thermally insulating acoustic separator for internal walls.

DOI: 10.15376/biores.19.4.9310-9333

Keywords: Hemp shiv; Crude glycerol; Low density board; Low energy binder; Particle board; Insulation board

*Contact information: a: Université LAVAL, Faculté de Foresterie, géographie et géomatique ◊· Département des sciences du bois et de la forêt, Pavillon Gene-H. Kruger, 2425 rue de la Terrasse, local 2342, Québec (Québec), Canada G1V 0A; b: Material Research Ltd, Unit 6, Forge Business Centre, Upper Rose Lane, Palgrave, IP22 1AP, UK; c: Suffolk Sustainability Institute, University of Suffolk, Waterfront Building, Neptune Quay, Ipswich, IP4 1QJ, UK; *Corresponding author: simon.pepin.1@ulaval.ca*

INTRODUCTION

There is an overwhelming need to decarbonise the built environment. The World Green Building Council (2022) has stated that buildings around the world must reach 40% less embodied carbon emissions by 2030 through urgent transformation. For net zero transformation of the sector, the availability and specification at design stage of low-carbon materials, lean low-carbon design, embracing digital technologies, decentralised energy generation and nature-based solutions are all vital (Royal Academy of Engineering 2021).

The use of plant-based materials in construction is growing in popularity in part because they sequester carbon during their growth phase through the action of photosynthesis, and this carbon is retained within the building for its life-time (Lawrence 2015). Parts from different plants have been used to produce eco-friendly building materials, including straw from different origins (Diaz Fuentes *et al*. 2020; Osvaldova *et al.* 2021; Quintana-Gallardo *et al.* 2021; Mucsi *et al*. 2022; Tlaiji *et al*. 2022), corn starch (Kulshreshtha *et al*. 2017) and stalks (Ahmad *et al*. 2018), reed stems (Albrecht *et al.* 2023)

and fibers (Silva *et al*. 2023), hemp fibers (Savas *et al.* 2024), and cotton (Wankhede *et al.* 2022; Kan *et al.* 2023). Nonetheless, timber and timber by-products are probably the most widely used plant-based material, and one major market segment is board materials such as plywood, oriented strand board (OSB), and medium density fibreboard (MDF). The most commonly used binder for these materials is a synthetic, petroleum-derived thermosetting adhesive, which is generally based on the reaction of formaldehyde with phenol, urea, melamine, or co-condensates (Dunky 2003). The use of formaldehyde as a binder is of particular concern because emissions from products manufactured using it are associated with serious health problems (Salthammer *et al*. 2010). Numerous studies have been undertaken to reduce the VOC emissions by decreasing the amount of free formaldehyde in the system, using formaldehyde scavengers, or replacing the adhesive with other adhesives, including bio-based adhesives (Hemmilä *et al.* 2017). These bio-based adhesives incorporate chemicals of different organic natures including proteins (Biancaniello *et al*. 2017; Xi *et al*. 2019; Mary *et al*. 2024a, b), sugars (Li *et al.* 2024; Liu *et al*. 2024), cellulose (Yang *et al.* 2023), lignin (Yuan *et al*. 2023), chitosan (Chen *et al.* 2023), and gum arabic (Zhao *et al*. 2023). Alternative adhesives that have been studied include crude glycerol (Bérubé *et al.* 2017; Segovia *et al.* 2021; Nitu *et al.* 2022). This is a solvent-free thermosetting adhesive based on an esterification condensation reaction under acidic conditions.

Crude glycerol is a by-product of the manufacture of bio-diesel, and it is from a renewable bio-based resource (Essoua Essoua *et al.* 2016). It has been estimated that for every 10 kg of bio-diesel produced, 1 kg of crude glycerol is created (Tisserat *et al.* 2012; Hu *et al.* 2012). Whereas valorising this requires additional refinement to create a chemically pure glycerol, Segovia *et al.* (2021) have shown that in its unrefined state, crude glycerol can be used as part of a thermosetting binding system. This offers a lower environmental impact for this by-product of the bio-diesel industry.

Citric acid is a weak organic acid present in vegetables and fruits, and it is obtained relatively inexpensively *via* fermentation (Soccol *et al.* 2006). Polymers derived from the esterification of glycerol and citric acid are relatively benign and biodegradable (Holser 2008). It has been shown that when citric acid is used to form ester cross-links with compounds having multiple -OH groups, the preferred reaction path involves more than one step (Nguyen and Pham 2020). The first step involves loss of one water from the citric acid, with the formation of a 5-membered anhydride ring, followed by a ring opening reaction a -OH group. The anhydride has been shown to have a lower activation energy for a subsequent esterification reaction with an -OH group. Because citric acid contains three carboxyl groups, the anhydride formation can then happen a second time. The second esterification reaction with another -OH group may result in crosslink formation between two different poly-alcohol groups.

The vast majority of studies using glycerol/citric acid binders to date have been focused on the creation of high density alternatives to particle board, in particular MDF. Segovia *et al.* (2020) used wood fibre to create boards with a target density of 785 kg/m^3, and Nitu *et al.* (2022) used jute particles to create boards with a target density of 900 kg/m^3. The present study explored the creation of lower density boards that might have potential for use as thermal insulating boards, using hemp shiv as the aggregate.

Hemp shiv is the woody core of the hemp plant (*Cannabis sativa*). Hemp grows rapidly with minimal requirement for fertilisers or herbicides, and it can be used as a break crop, which also has the advantage of improving soil structure (European Commission 2023). Once harvested, the hemp stem undergoes retting followed by mechanical

defibrillation, separating the outer bast fibre from the inner woody core, known as shiv. Hemp shiv has a very low density and thermal conductivity due to its porous structure (Hussain *et al.* 2019) and has been traditionally combined with a mineral binder to create a low density bio-composite known as hemp-lime or hempcrete.

The present work used hemp shiv and a bio-based adhesive made of crude glycerol and citric acid to produce hard insulating boards. The physical and hygrothermal properties such as density, thickness swelling in the presence of moisture, water absorption, water vapour transmission, dynamic vapour sorption, thermal conductivity, and acoustic properties, as well as mechanical properties such as compressive strength and bending properties, were evaluated. The microstructure of the composite was examined using scanning electron microscopy (SEM).

EXPERIMENTAL

Materials

Crude glycerol, which was previously characterized by Segovia *et al.* (2020), was obtained from Rothsay Biodiesel (Cambridge, Canada) and filtrated under vacuum with a grade 4 Whatman filter paper before use. Anhydrous citric acid (≥ 99.5%), p-toluenesulfonic acid (p-TSA, ≥ 98.5%), and corn starch were purchased from Sigma-Aldrich (St-Louis, MO, USA). A sodium silicate adhesive (Na_2O = 9.0%, SiO_2 = 29.0%) was obtained from The Pottery Supply House, Oakville, Canada, and a two-parts polyurethane structural adhesive, Loctite® Purbond GT20 + Loctite® Purbond GT205, was obtained from Henkel (Mississauga, Canada).

This study used Kanabat hemp shives (Fig. 1) produced by La Chanvrière (St-Lyé, France) and supplied by NovEnviro (Québec, Canada), without any drying or modification. They were characterized following the RILEM TC 236-BBM recommendation (Amziane *et al.* 2017), and the results are presented in Table 1. The initial moisture content and bulk density were determined following 24 h of oven drying at 103 °C. The particle size distribution was assessed by the image analysis method, where 600 dpi images were obtained with a WinDENDRO^{TM} LA1600 scanner (Régent Instruments Inc, Québec, Canada) and analyzed with ImageJ (LOCI, Madison, WI, USA).

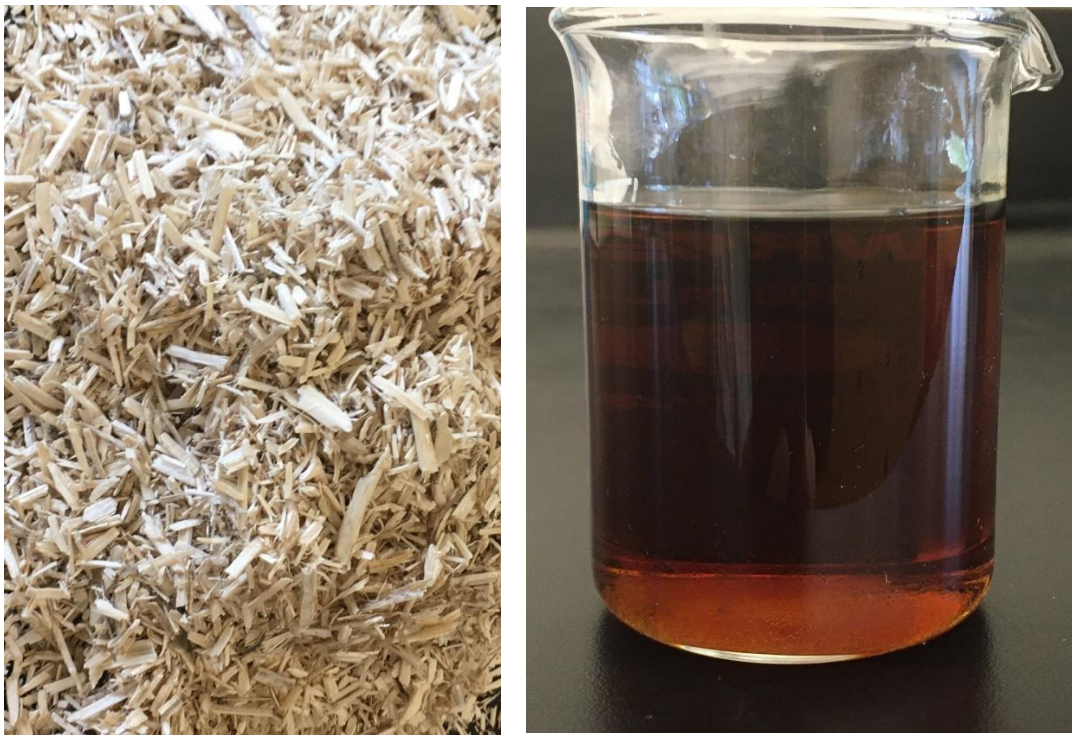

Fig. 1. Hemp shiv and GC-CA adhesive used in the study

Table 1. Characterization of the Hemp Shives

Initial moisture content (%)	Bulk density (kg/m^3)	Length (mm)			Width (mm)		
		Min	Max	Av.	Min	Max	Av.
8.78	112	0.92	32.39	7.64	0.39	5.39	1.91

Methods

Preparation of the crude glycerol (CG) and citric acid (CA) adhesives

Based on the procedure by Segovia *et al*. (2020), the adhesives were prepared by heating CG and CA under stirring, in a molar ratio of 1:0.66, at a temperature of 95 °C for 2 h. Following the complete dissolution of CA, the heat was turned off and 1.33% m/m of p-TSA was added to the mixture as an acidic catalyst (Berube *et al*. 2018), while stirring for an additional 15 min. Then, the beakers were covered and cooled overnight. Corn starch (CS) was added to some cooled adhesives in an appropriate amount so that, once the adhesives are mixed with the hemp shiv, it would represent 0%, 5%, or 10% of the total mass of the preparations. To reduce the viscosity of the adhesives, they were diluted with 25% m/m of water.

Preparation of the panels

Prior to mixing, the adhesives were heated to 65 °C to further decrease their viscosity. Using a constant 6:1 ratio by mass between the particles and the GC-CA mix, the adhesives were combined with the hemp shives in a rotating drum tank equipped with a pneumatic atomizer. Table 2 describes the dry composition of each preparation.

Table 2. Mass of Hemp Shiv, Adhesive (GC + AC), and Corn Starch for 100 g of Preparation

Corn Starch Content (%)	Hemp Shiv (g)	Adhesive (g)	Corn Starch (g)
0	85.7	14.3	0.0
5	81.4	13.6	5.0
10	77.1	12.9	10.0

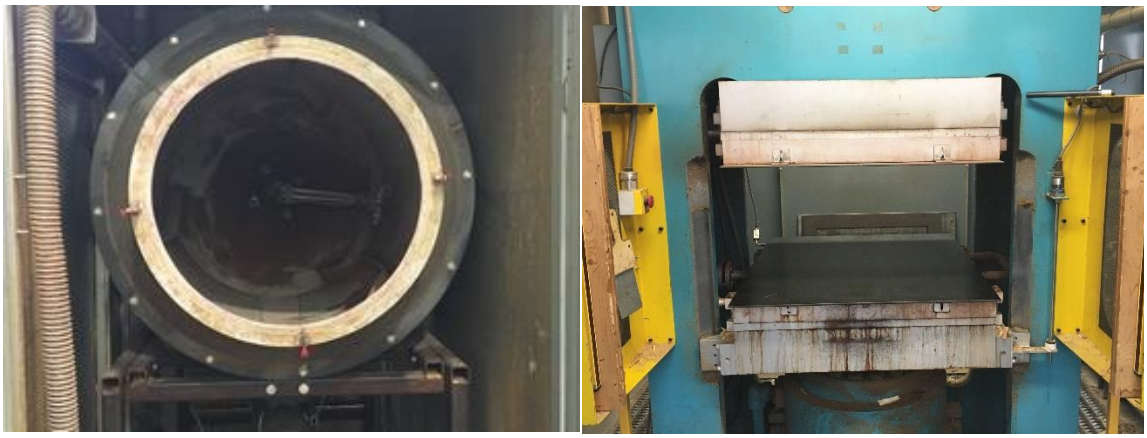

Fig. 2. Rotating drum and hot press used to prepare the panels

For each preparation, 10 panels with target densities of 250 and 300 kg/m^3 were produced by adding 1500 g and 1975 g of preparation to a 46 cm x 56 cm mold. After forming a mat by hand, the mold was removed and the mat was directly pressed in a hot press (Dieenbacher, Alpharetta, GA, USA) to a thickness of 18 mm at 200 °C for 17 min. Because of the low density of the panels, no actual pressure was held on the mats as the adhesive cured, the hot press simply maintaining their thickness at the desired dimension. After cooling overnight, the panels were cut to 41 cm x 53 cm, and a 7.6 cm x 53 cm strip was sampled for the static bending test. The panels were then laminated into 2-ply, 36 mm thick boards by spreading 300 g/m^2 of sodium silicate adhesive on the top panel and holding a pressure of 475 kPa for 30 min at ambient conditions. The different boards prepared were identified according to their target density and corn starch content, as presented in Table 3.

Table 3. Identification of the Panels Used in the Study

Identification	Target Density (kg/m^3)	Corn Starch Content (%)
250	250	0
250-5	250	5
250-10	250	10
300	300	0
300-5	300	5
300-10	300	10

The laminated boards were finally sawn into the different samples required for the tests and conditioned at 23 °C and 50% relative humidity for at least 7 days before testing. One sample was cut from each board for each test, except for the density profile, which sampled two opposite corners and the middle of each board. The dimensions of the samples

are presented in Table 4. As the glue line with sodium silicate was too weak and was found to fail during the compressive strength test, new samples were prepared using 200 g/m^2 of Purbond polyurethane adhesive and a pressure of 345 kPa for 3 h.

Table 4. Information on the Samples for Each Test

Test	Dimensions (cm)	Repetitions
Density profile	5 x 5 x 3.6	15
Thermal conductivity	25 x 25 x 3.6	5
Moisture buffering	10 x 10 x 3.6	3
Water absorption and thickness swelling	15 x 15 x 3.6	5
Water vapor transmission rate	10 x 10 x 3.6	3
Dynamic vapor sorption	1 shiv	3
Static bending	7.6 x 53 x 1.8	10
Compressive strength	2.5 x 10 x 3.6	5
Acoustic properties	4.4	5

Characterization of the panels

Panels 250, 250-10, 300, and 300-10 were examined by scanning electron microscopy (SEM) with a FEI Quanta 250 microscope (FEI Company Inc. Thermo-Fisher Scientific, Hillsboro, OR, USA) under an acceleration voltage of 15 kV. To increase their conductivity, a thin layer of Pd/Au coating was deposited on the analyzed surfaces.

The density profile of the boards was analyzed along the thickness with a model QDP-01X X-rays densitometer (Quintek Measurement Systems Inc., Knoxville, TN, USA). A measurement was made every 0.04 mm and the moisture content (MC) of the samples was subsequently calculated with Eq. 1,

$$MC\ (\%) = \frac{(m_2 - m_1)}{m_1} \cdot 100\% \quad (1)$$

where m_1 and m_2 are the oven dried (103 °C for 24 h) and conditioned masses of the samples, respectively.

Thermal conductivity

The thermal conductivity of the boards was evaluated following the ASTM C518-21 (2021) standard using a LaserComp Fox314 heat flow meter (TA Instruments, Wakefield, MA, USA) equipped with a Thermo Cube cooling system (Plymouth, IN, USA) and their Wintherm32v3 software. The samples were placed between a cold plate (T = 10 °C) and a hot plate (T = 35 °C), for an average temperature of 22.5 °C and a ΔT of 25 °C. The steady state was considered attained when the thermal conductivity λ varied by less than 0.5% over 45 min.

Hygric properties

The moisture buffer capacity of a material allows it to moderate fluctuations in the relative humidity of an enclosed space by utilizing the adsorption/desorption properties of the material. In addition to stabilizing internal environmental conditions, it also helps to minimize surface condensation.

The moisture buffer value of the materials was evaluated using the method proposed by Rode and Grau (2008). Test specimens, sealed on five sides, were exposed to repeated step changes in ambient relative humidity at a constant temperature of 23 °C. The mass change of the specimen was monitored at 30 sec intervals. Specimens were conditioned at

23 °C, 50% RH until there was less than 0.1% mass change between two successive daily determinations. The moisture buffer value can be classified within the 'practical moisture buffer value classes' consisting of the following ranges – negligible; limited; moderate; good; and excellent (Rode and Grau 2008).

The climate chamber used was a Memmert HPP110eco, and the scales were A&D EJ-1202 max 1200 g, d=0.001 g. Test conditions were 8 hours at 75%RH followed by 16 hours at 33%RH. Cycles were repeated until the difference between mass gain and mass loss between each cycle were <5% of Δm.

The dynamic vapor sorption (DVS) analysis was performed on a DVS Adventure water vapor analyzer (Surface Measurement Systems, Allentown, PA, USA) using their DVS Control software. For each treatment presented in Table 5, a single hemp shiv (m = 15 mg) was selected for the analysis. In both the absorption and desorption curves, the sorption isotherm included all the steps between 0% and 95%, with 10% ± 0.1% increments. For each step, the equilibrium moisture content (EMC) was considered reached when the $\Delta m/\Delta t$ was lesser than 0.002% over 10 min. The temperature was held at 25 ± 0.02 °C for the whole duration of the analysis.

Table 5. Treatments Used for the Water Sorption Analysis

Treatment Name	Adhesive	Hot-pressed	Corn Starch Content (%)
Hemp Shiv	No	No	0
Adhesive	Yes	Yes	0
Starch	Yes	Yes	10

The water absorption and thickness swelling tests were performed following the ASTM D1037-12 (2020) standard. Samples previously dried at 103 °C for 24 h were submerged in de-ionized water (T = 23 °C), and their mass was measured to the closest 0.01 g after 15 min, 1 h, 2 h, 4 h, 8 h, and 24 h. Before each measurement, the samples were allowed to drip for 5 min to remove the excess free water and the surfaces were patted dry with paper towels. For each step, the moisture content was calculated with Eq. 1. After each weighing, the thickness of the samples was also measured at 12 different points (each corner plus two measurements on each side) to the closest 0.01 with an Absolute Digimatic digital caliper (Mitutoyo, Aurora, IL, USA). For each step n, the thickness swelling was calculated as follows,

$$TS\,(\%) = \frac{T_n - T_1}{T_1} \cdot 100\% \quad (2)$$

where T_1 and T_n are the mass of the oven dried and soaked sample, respectively.

The water vapor transmission rate (WVTR) was assessed following the guidelines of the ASTM E96-22a standard. The samples were placed over 10 cm x 10 cm Plexiglas boxes containing either de-ionized water (wet cup) or a $CaCl_2$ desiccant (dry cup). The sides of the samples were sealed with an aluminium tape to only allow the flow of water vapor through the top surface. The assemblies were kept in a conditioning chamber at 23 °C and 50% relative humidity (RH) for the whole duration of the experiment, about two weeks. During the first week, the specimens were simply laid to rest to approach the steady state. From the second week, they were weighted on a digital scale (± 0.002 g) twice per day and their mass was plotted against the time until it would reach a constant variation for at least 6 consecutive weightings, indicating the steady state. The normalized WVTR was then calculated with Eq. 3,

$$NWVTR\ (g/h \cdot m)\ =\ \frac{(G/t)}{A} \cdot T \quad (3)$$

where *G/t* is the slope of the variation of the mass of the assemblies at steady state in function of time (g/h), *T* the thickness of the boards (m), and *A* is the exposed surface of the sample (m^2).

Mechanical properties

The flexural strength and the compressive strength parallel to surface were assessed in accordance with the ASTM D1037-12 (2020) standard using a MTS QTest/5 universal testing machine (MTS System Corporation, Eden Prairie, MN, USA). The modulus of rupture (MOR) and modulus of elasticity (MOE) were determined with the static bending test using a 432 mm span and a rate of head descent of 8.5 mm/min. They were calculated as follows,

$$MOR\ (MPa)\ =\ \frac{3PL}{2bd^2} \quad (4)$$

$$MOE\ (MPa)\ =\ \frac{(L^3)}{4bd^3} \cdot \frac{\Delta P}{\Delta y} \quad (5)$$

where *P* represents the maximum load (N), *L* the length of the span (mm), *b* the width of the sample (mm), *d* the thickness of the samples (mm), and *ΔP/Δy* the slope of the straight line portion of the load-deflection curve (N/mm). The compressive strength, R_c, was determined with the compression parallel to the surface test using a rate of head descent of 0.5 mm/min and calculated by Eq. 6,

$$R_c\ (kPa)\ =\ \frac{P}{A} \quad (6)$$

where *P* represents the maximum load and A the area of the sample.

Acoustic properties

The normal incident transmission loss and absorption coefficient, between 117 Hz and 4322 Hz, were evaluated with a 44.44 mm impedance tube from Mecanum Inc. (Quebec, Canada) and their Tube-X software. The method, based on the ASTM 2611-19 standard, used 3 microphones; two between the signal generator and the sample, and one behind the sample. To obtain the normal incident transmission loss, two measurements, with 30 mm and 60 mm air cavities between the sample and the third microphone, were taken. The absorption coefficient on a hard wall was simulated by the Tube-X software.

Statistical analysis

A statistical analysis was performed on the results of the mechanical properties tests, as well as the water absorption and thickness swelling after 24 h. RStudio (Posit BPC, Boston, Massachusetts, USA) was used to perform a Tukey HSD with $\alpha = 0.05$, and the difference between two types of boards was considered significant when $p < 0.05$.

RESULTS AND DISCUSSION

Characterization of the Panels

SEM

Samples of shiv before and after applying the binder were examined under SEM (Fig. 3.) Two specimens with very similar morphology were identified. The left-hand image shows a section through the length of a piece of shiv. Running diagonally across this image can be seen a line of perforations about 15 µm long and 2 µm wide. A similar line in the right-hand image (shiv coated with binder) shows the perforations to have been occluded by the binder.

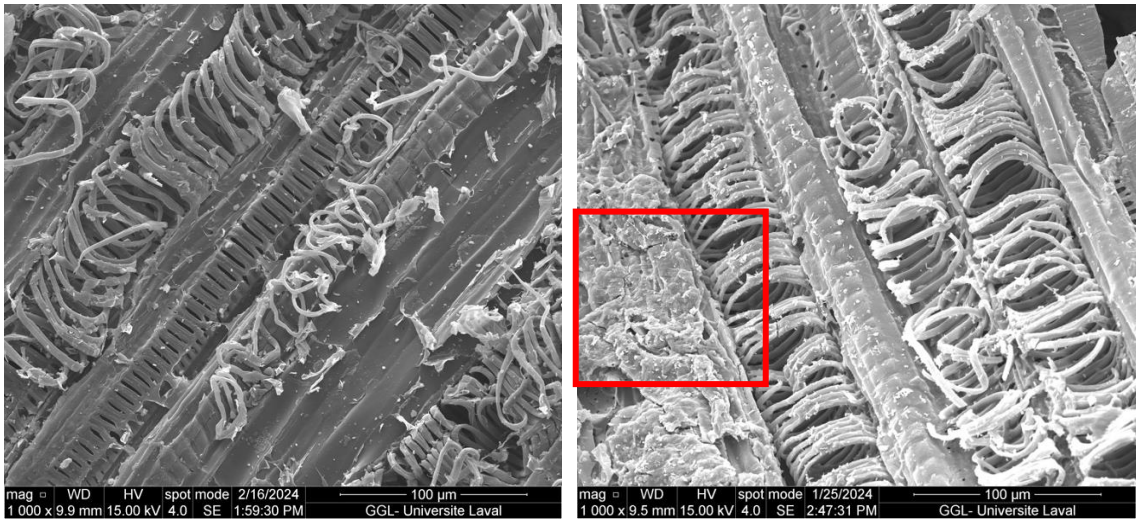

Fig. 3. SEM Images of hemp shiv (left) and hemp shiv with binder (right)

A close-up of the lower left-hand side of this image (outlined) shows a thin layer of binder (Fig. 4) covering the surface of the shiv. This layer is sub 1 µm in thickness and is cracked in places due to the brittle nature of the binder.

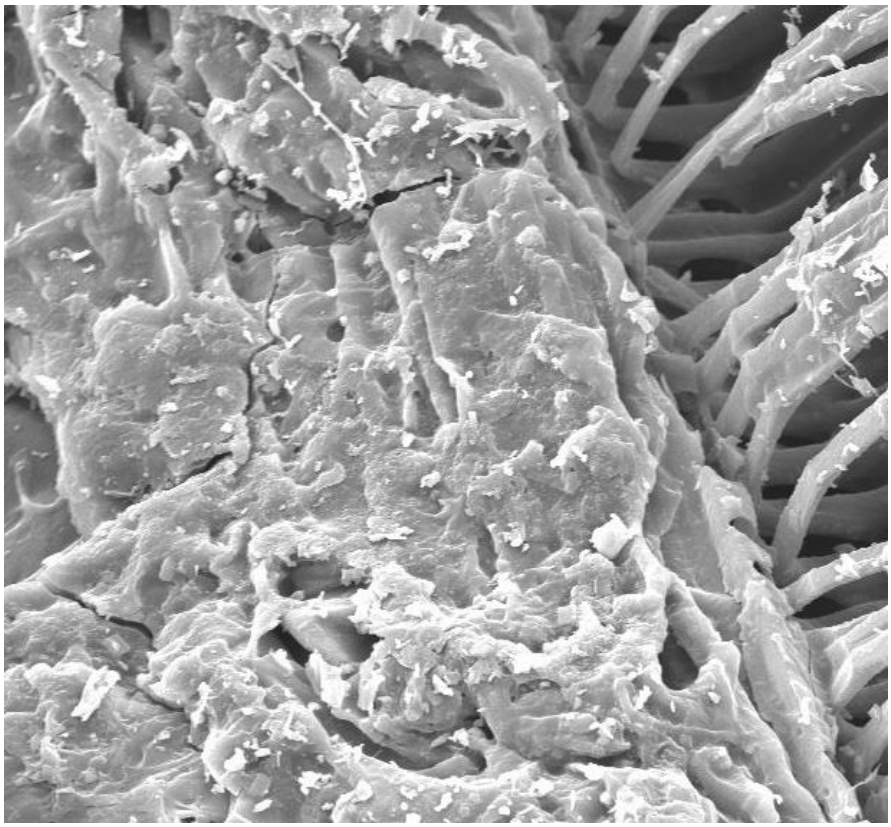

Fig. 4. Close-up of section of shiv with binder showing binder with cracks

A cross-section of the end of a piece of shiv that has been coated in binder (Fig. 5) shows the pith layer consisting of aligned parenchyma cells with diameters of the order of 10 to 50 μm, where the majority of these openings have not been occluded by the binder.

The conclusion that can be drawn from these images is that although larger pores were not occluded by the binder, pores below ~1 to 5 μm can become occluded, which will reduce the overall porosity of the composite. The effect of this reduction in porosity can be quantified by comparing the moisture buffering of the composite with the moisture buffering of hemp-lime where small pores are not occluded (Latif *et al.* 2015). This is discussed in a later section of this paper.

Density profile

The average density of the boards and their respective moisture content are presented in Fig. 6, while their density profiles along the thickness are presented in Fig. 7. Though a quick look at Fig. 6 indicates that the boards exceeded their target densities of 250 and 300 kg/m^3, a closer look at their density profiles indicated that most of the thickness of the boards was actually very close to or even below their target density while being denser toward the surfaces. This was however not the case for the 300-10 samples, which were denser than the target along all their thickness. The density did increase toward the edges of each panels used to manufacture the boards, where the hemp shiv mats were pressed and heated. This observation is particularly true for the 300 kg/m^3 samples, which attained densities over 400 kg/m^3.

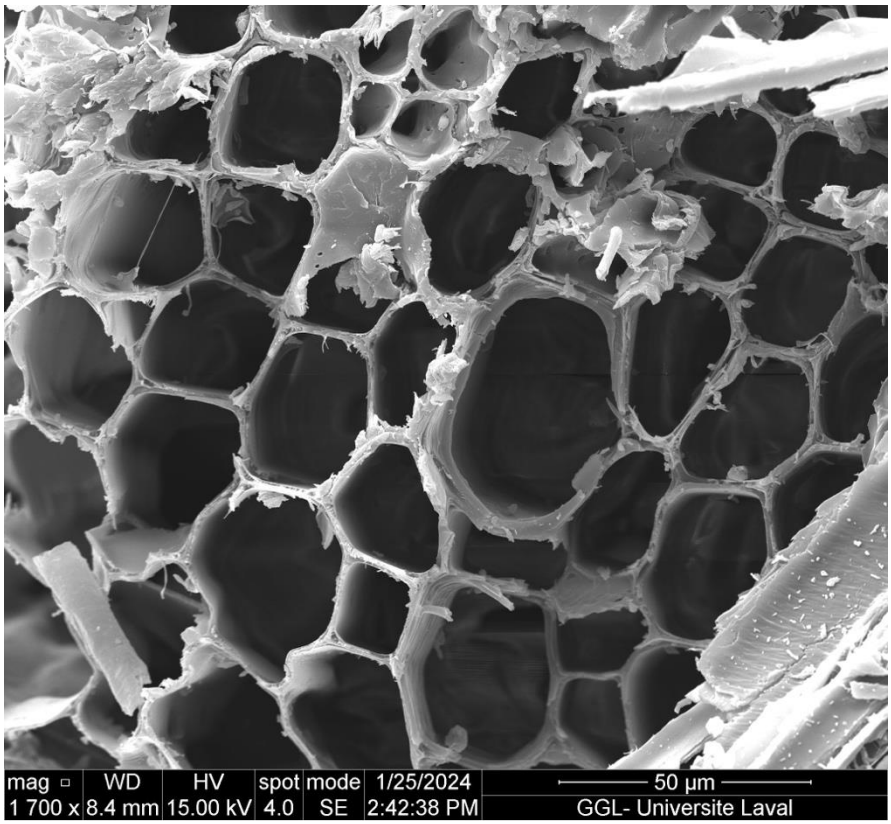

Fig. 5. Cross-section of coated shiv in the pith layer showing parenchyma cells

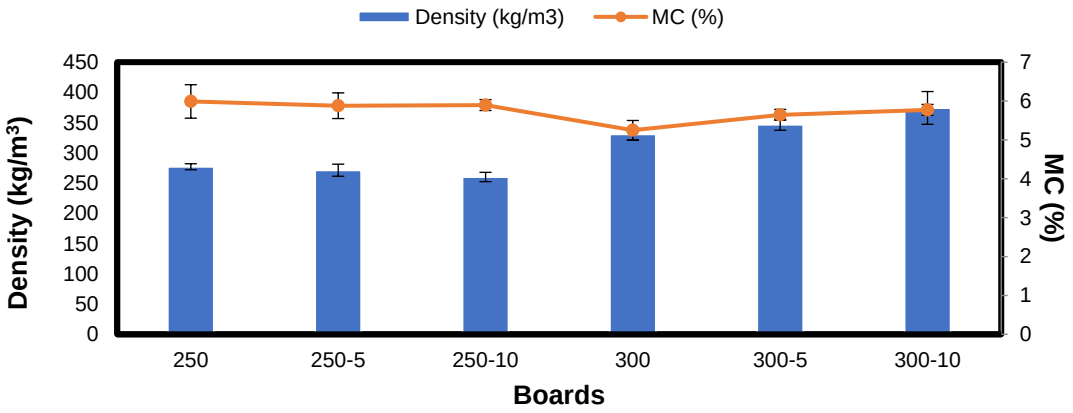

Fig. 6. Density and moisture content (MC) of the hemp shiv boards

Nonetheless, the sodium silicate adhesive is responsible for most of the excess density, with a large peak reaching 650 kg/m^3. Since the spread rate of the adhesive was the same for every board, it can however be determined that the difference of density between the different boards remains exact. From the shape of its curve in Fig. 7, it can be estimated that low density of the panels allowed the sodium silicate adhesive to penetrate within the boards by approximately 2 mm on each side of the glue line.

Although the 300 boards had a slightly lower MC than the other boards, neither the density of the boards or the corn starch content seemed to have had an impact on the EMC.

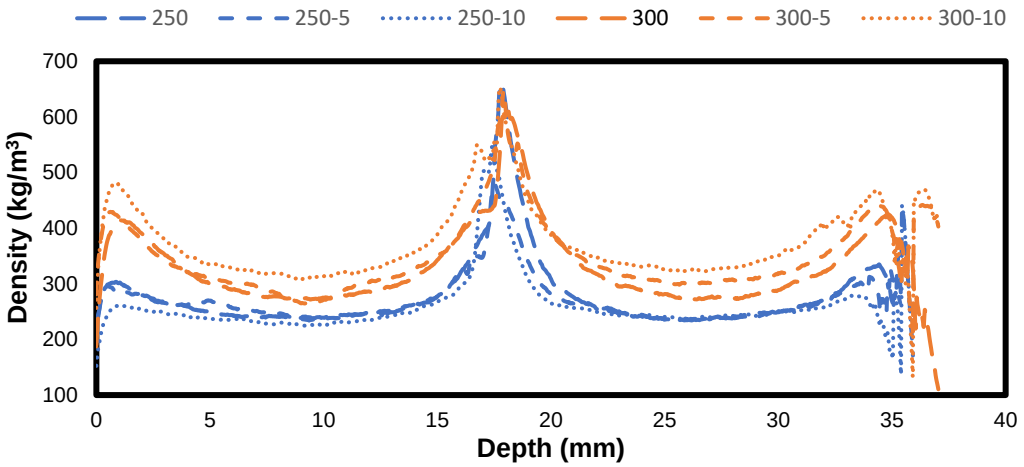

Fig. 7. Density profile along the thickness of the hemp shiv boards

Thermal Conductivity

The thermal conductivity of the studied boards is presented in Fig. 8. The thermal conductivity of the 250 kg/m^3 boards, between 0.0693 and 0.0699 W/mK, was slightly inferior to the 300 kg/m^3 boards, ranging from 0.765 to 0.783 W/mK. By comparing this graph to Fig. 6, it can be observed that the density of the boards was the leading factor influencing the thermal conductivity. It is evident that the amount of corn starch present in the boards had a negligible impact on their thermal conductivity.

Hemp-lime composites tend to have higher densities than the materials studied here, but a review of lower density hemp-lime composites (around 300kg/m^3) shows thermal conductivities of the order of 0.08W/m.K (Barbhuiya and Das 2022), which are marginally higher than those tested here, probably due to the difference in thermal conductivity of the binder.

The particle board had a significantly lower thermal conductivity than the current range of particle boards at 0.07 W/m.K compared with 0.13 W/m.K for boards currently available on the market.

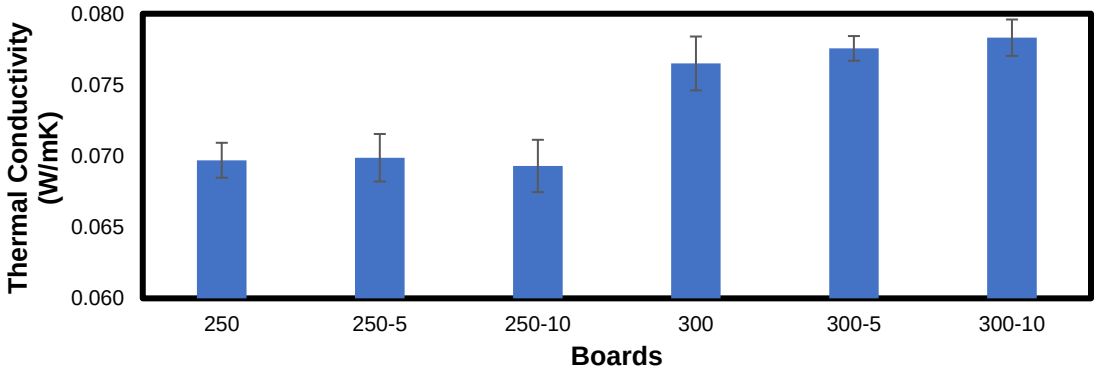

Fig. 8. Thermal conductivity of the hemp shiv boards

Hydric Properties

Moisture buffering

The moisture buffer values (MBV) for the boards were measured at 1.73 g/m^2/%RH for the 250 specimen and 1.68 g/m^2/%RH for the 300 specimen (Fig. 9). This places both specimens at the higher level of 'good' moisture buffering capacity (Fig. 10).

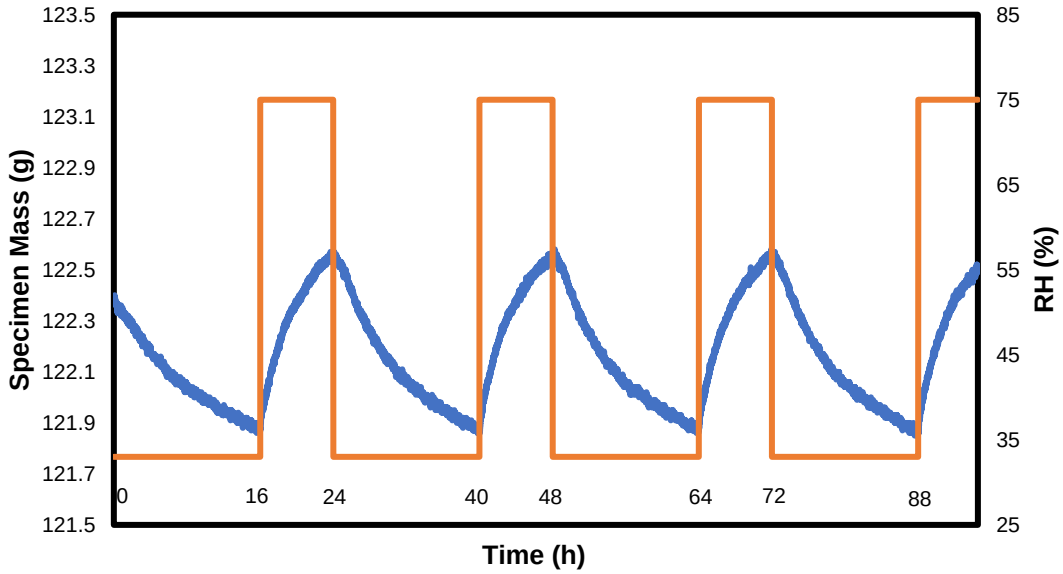

Fig. 9. Moisture buffer data for 300 specimens

This is lower than hemp-lime which typically has a value of 3 to 3.5 g/m^2/%RH (Latif *et al.* 2015), but still has the potential to contribute to maintaining a good level of indoor air quality. The reason for this reduction in MBV is due to the binder having occluded small pores (1 to 5 µm) in the system, decreasing the overall porosity (Figs. 3, 4, 5).

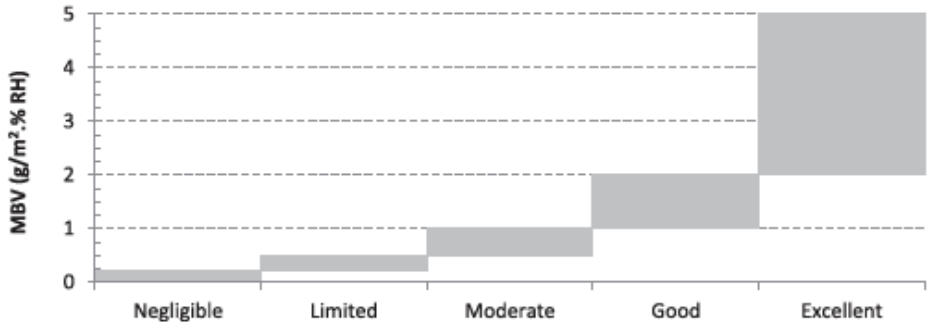

Fig. 10. Moisture buffer classes

Dynamic vapor sorption (DVS)

The sorption isotherms of the raw hemp shives, the pressed shives covered with adhesive, and the pressed shives with adhesive and 10% of corn starch are presented in Fig. 11. An important decrease in the equilibrium moisture content (EMC) is noticeable between the Shiv and Adhesive curves, with EMC at 95% RH of 20.41% and 15.78%, respectively. This diminution in hygroscopicity can be attributed to the degradation of the polysaccharide components of the hemp shives (cellulose and hemicelluloses) during the hot pressing, as

their decomposition begins around 200 °C (Diakité *et al*. 2021). The addition of corn starch does not substantially affect the hygroscopicity of the pressed shives at lower relative humidity levels, which may explain the low variability in MC of the boards presented in Fig. 6. However, an important surge in water adsorption can be observed at RH above 60%, with an EMC of 18.42% at 95% RH.

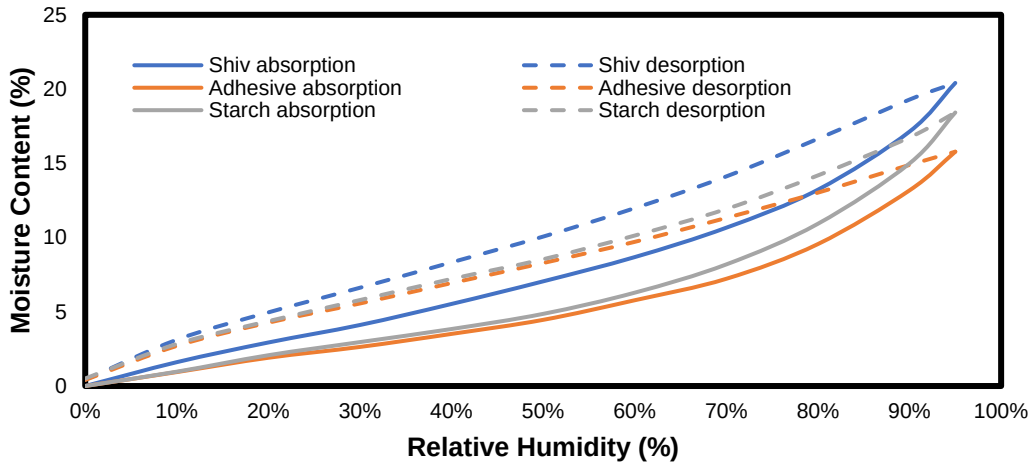

Fig. 11. Sorption isotherms for the raw hemp shives (Shiv), pressed shives covered with adhesive (Adhesive), and pressed shives with adhesive and 10% of corn starch (Starch)

Water absorption and thickness swelling

The water absorption and thickness swelling during full immersion of the boards in water are presented in Fig. 12, and their corresponding Tukey HSD are displayed in Table 6. Both graphs show a very rapid increase during the first 15 min of immersion, as free water penetrates into the voids of the low density boards, followed by a slower progression over the rest of the test period, as it diffuses into the cell wall of the hemp shives. By comparing these two graphs, it seems that the water absorption and thickness swelling were not perfectly correlated. For example, the 250-10 boards absorbed more water, but they swelled less than the 250 ones.

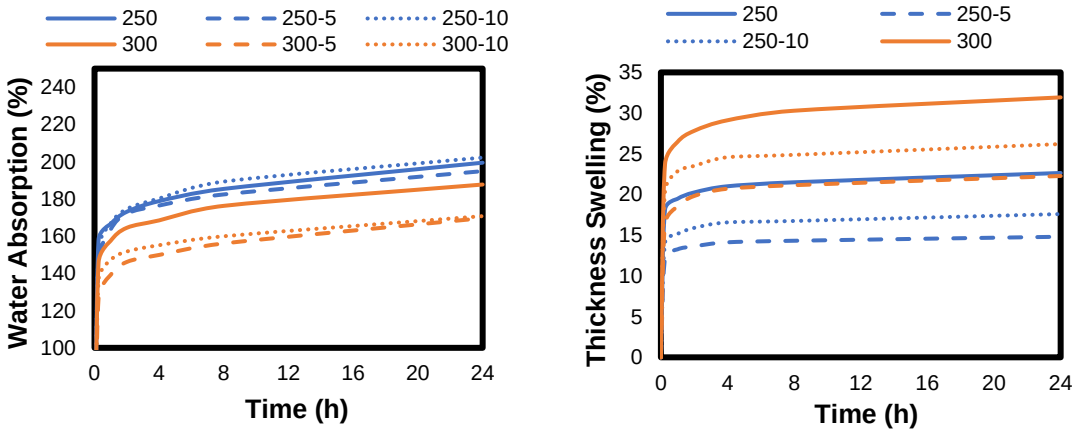

Fig. 12. Water absorption (left) and thickness swelling (right) of the hemp shiv boards during full immersion in water

Table 6. Tukey HSD of the Water Absorption and Thickness Swelling after 24 h

Boards	Water Absorption (%)	Thickness Swelling (%)
250	199.45a	22.64ab
250-5	198.12a	15.01b
250-10	202.22a	17.60b
300	187.72ab	31.93a
300-5	169.67b	22.27ab
300-10	170.75b	26.20ab

Different letters indicate a statistical difference.

In general, the 250 kg/m^3 boards absorbed more water than the 300 kg/m^3 ones, but they had a lower thickness swelling. While it would certainly be logical that the 250 kg/m^3 boards absorbed more water, as they contain more voids for water to fill (Fig. 13), and that it is true in a sense, as their percentages of weight gain are slightly higher, these boards absorbed less water than the 300 kg/m^3 ones (Table 7). A fraction of this difference could lie in the bound water difference, as the 300 kg/m^3 boards contain more hemp shives for the same volume. However, with fiber saturation points between 15.8% and 18.4% (Fig. 11) and a dry mass difference of approximately 40 g between the samples of each density groups, less than 8 g of water absorption can be explained as being bound water.

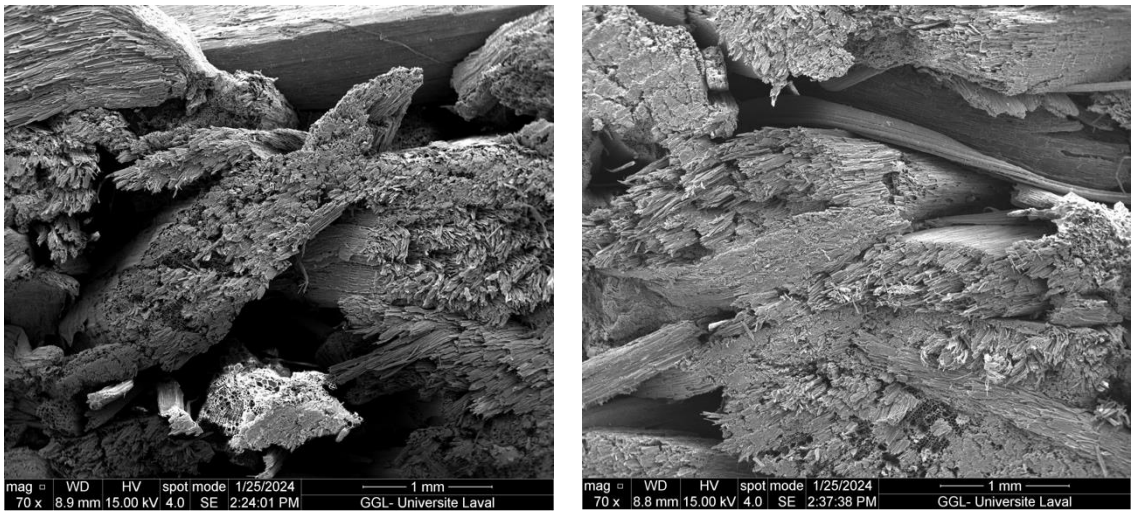

Fig. 13. Void spaces in 250 (left) and 300 (right) specimens

Therefore, despite having less voids in their structure, the 300 kg/m^3 boards absorbed more free water than their 250 kg/m^3 counterparts. Thus, it can be concluded that an important proportion of the difference between the swelling of the two density groups is induced by some spring-back rather than the swelling of the cell wall of the hemp shives. However, the latter is not completely negligible, as the swelling rate of the 300 kg/m^3 boards, during the last 12 hours, was twice as important as the 250 kg/m^3 boards. This observation could be attributed to the lower void volume inside the 300 kg/m^3 boards, which forces the swelling of the hemp shiv outward.

Table 7. Mass of Water (g) Absorbed in 24 h by the Boards during Full Immersion

250	250-5	250-10	300	300-5	300-10
419.57 (13.66)	408.83 (13.13)	427.57 (10.65)	470.15 (15.25)	451.34 (22.87)	454.78 (29.95)

Note: Standard deviation is in parentheses

The corn starch does not seem to have had a clear impact the water absorption of the boards. However, it seems to affect their thickness swelling, as both density groups followed a trend of 0% > 10% > 5%. As shown below in the mechanical properties (Fig. 16), the addition of 5% of corn starch increased the MOE of the boards, which may have reduced their spring-back. However, increasing its concentration to 10% did not really add any more strength to the boards, but may increase its sensitivity to moisture.

Water vapor transmission rate (WVTR)

The normalized WVTR for both the wet cup and the dry cup tests are presented in Fig. 14. A clear reduction of the WVTR was observed when the density of the boards was increased from 250 to 300 kg/m^3, as the void space within the boards diminished and the passage of moisture was hindered. Contrastingly, the effect of the corn starch was rather vague. For the 250 kg/m^3 boards, the wet cup WVTR was slightly reduced as the corn starch content increased, while their dry cup WVTR increased; in the case of the 300g/m^3 boards, the opposite was observed. The effect of the corn starch could however be negligible, as a good connection can be found between WVTR shown in Fig. 14 and the density of the boards shown in Fig. 6. In the case of the dry cup, an inverse relationship exists between the density of the boards and their WVTR, which is coherent with the tendencies observed between the two density groups. For the wet cup, however, it was demonstrated by other authors that surface diffusion occurs when RH conditions are near saturation (Albaalbaki and Hill 2012). The surface diffusion, which is more important as the surface area increases, artificially inflates the values of WVTR. This may explain why, as the density of the boards increases, the wet cup WVTR also increased. Still, this should only be valid if, past a certain density, the surface diffusion grows faster than the water vapor transmission's reduction. From the wide range of WVTR rates presented, it seems evident that the WVTR kinetics is governed by the hemp shiv panels and that the layer of sodium silicate adhesive does not resist the transmission of moisture.

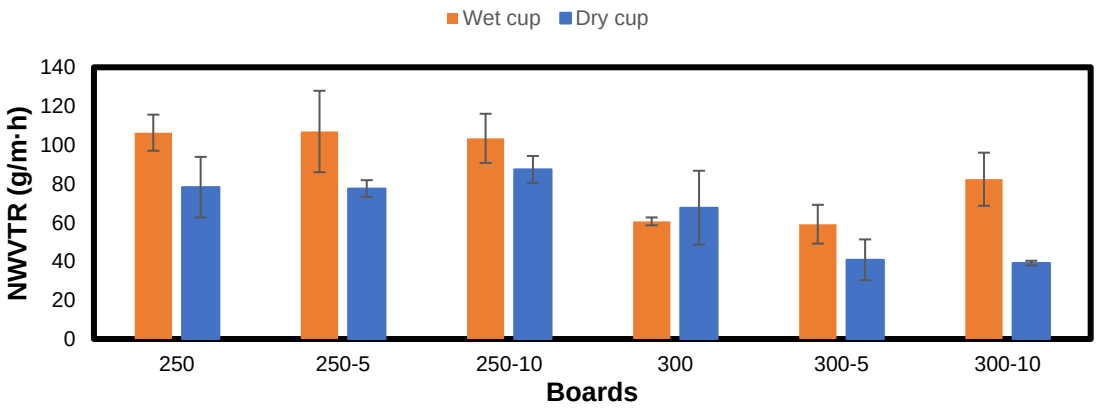

Fig. 14. Normalized water vapor transmission rate (NWVTR) of the hemp shiv boards over wet and dry cups

In addition to the WVTR analysis, a water vapor resistance factor was calculated following BS EN ISO 12573:2016 using the dry cup method (Fig. 15). This factor (μ) is widely used in the construction industry and indicates how much greater the resistance of the material is compared to an equally thick layer of stationary air at the same temperature. Oriented strand board, for example, has a μ value of 430 (dry cup) (Smartply Ultima data sheet 2024), and hemp-lime blocks have a corresponding value of 3 (IsoHemp 2024). Compared with most board materials, this material is highly vapour permeable, which makes it suitable for applications needing high vapour permeability and moisture buffering.

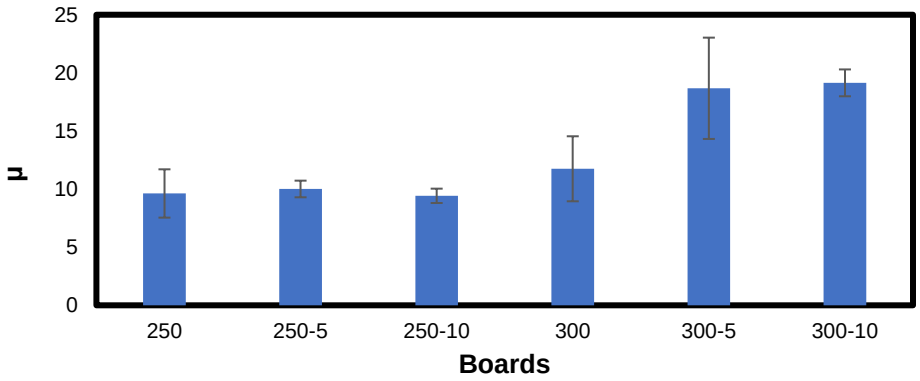

Fig. 15. Water vapour resistance factor (μ)

Mechanical Properties

The MOE, MOR and compressive strength of the studied boards are presented in Fig. 16. In each case, an increase in the density of the boards yielded a higher strength.

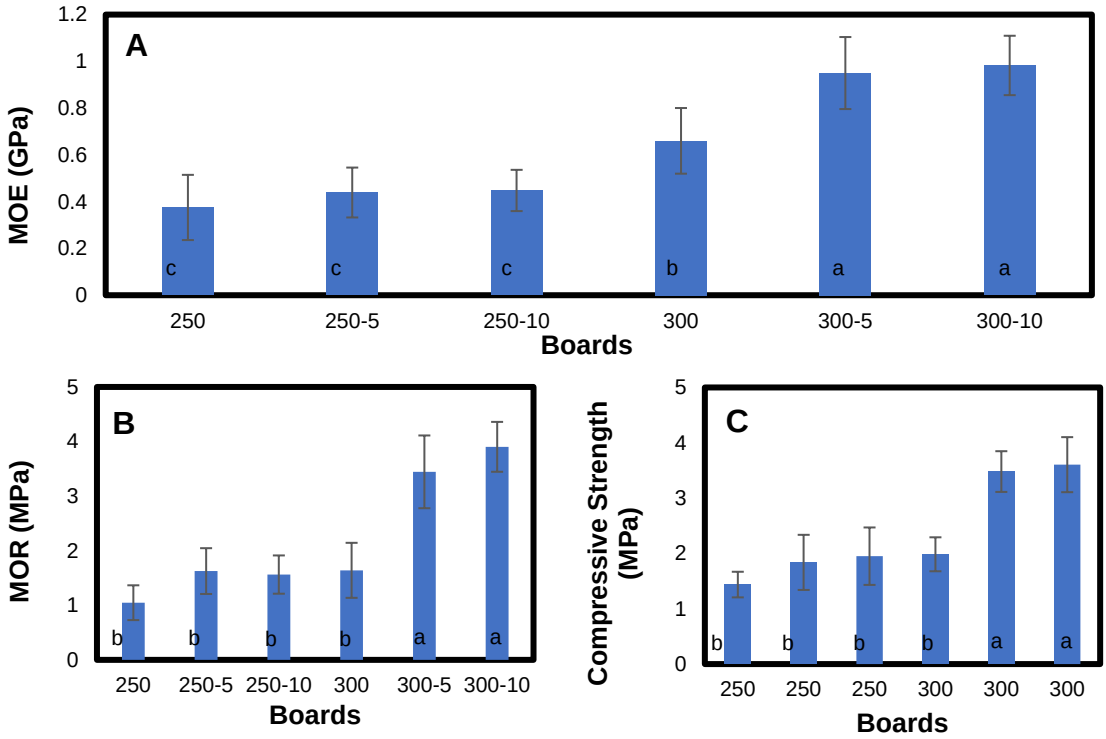

Fig. 16. A) Modulus of elasticity (MOE), B) modulus of rupture (MOR), and C) compressive strength of the hemp shiv boards. Letters correspond to the Tukey HSD analysis.

Likewise, the first 5% of corn starch increased the mechanical properties of the tested boards, particularly at 300 kg/m^3. It suggests that, while corn starch did improve the bonding of the hemp shives, a 250 kg/m^3 density may lack the contact surface (Fig. 13) to benefit substantially from an improvement in adhesion. Increasing the amount of corn starch to 10% resulted in only a very small gain in mechanical strength, hinting that the effect of corn starch caps quite rapidly.

These materials have a markedly higher compressive strength than hemp-lime composites of a similar density, which are in the range of 0.20 to 0.35 MPa for densities between 250 and 300 kg/m^3. In comparison with a typical MDF board (ρ of 600 kg/m^3), these materials are considerably weaker, since a standard grade MDF board would be required to have an MOR value of 13 MPa and an MOE value of 1.2 GPa. (Segovia *et al.* 2020). It is clear that these materials are not capable of being a like-for-like substitute for MDF, but they do have the potential to act as insulation boards or non-structural insulating render carriers.

Acoustic Properties

The normal incident transmission loss and absorption coefficient of the hemp boards, between 117 and 4322 Hz, are shown in Fig. 17, and the average values over this range are presented in Table. 8. Thanks to their low density and high thickness, the boards had both decent transmission loss values and absorption coefficients.

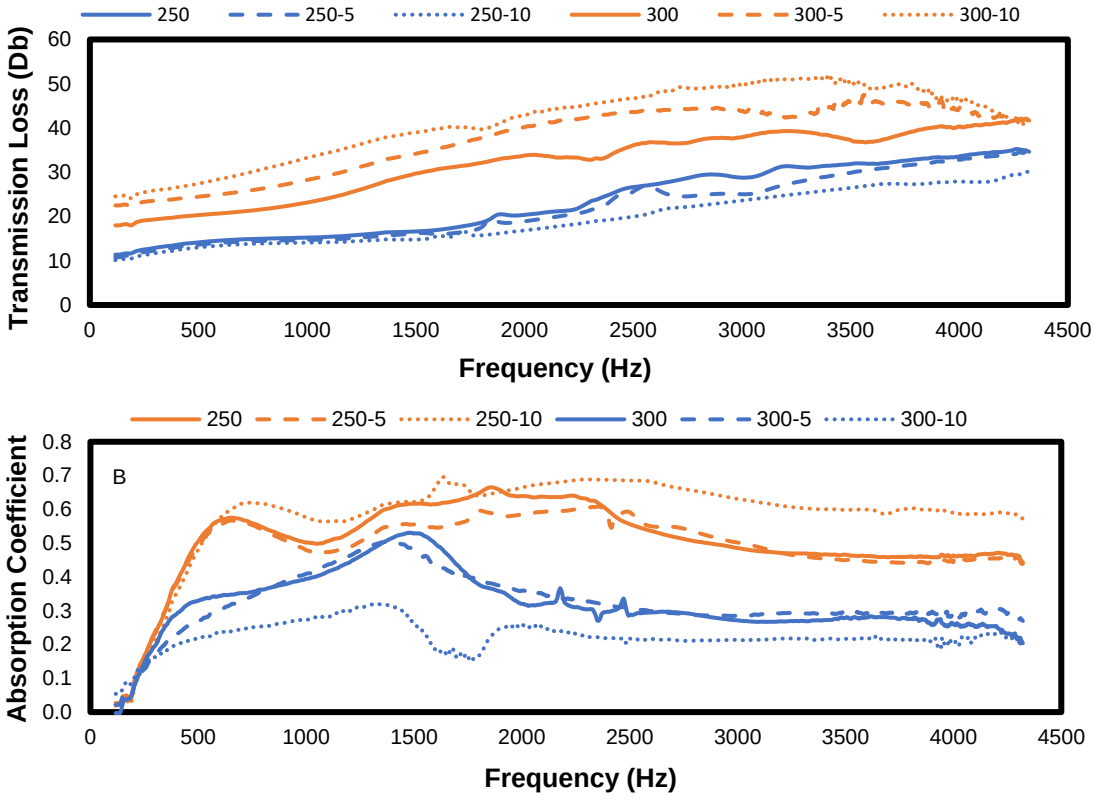

Fig. 17. A) Normal incident transmission loss and B) absorption coefficient of the hemp shiv boards

According to the mass law, a higher density material would result in a higher transmission loss (Cowan 2014). This is quite evident in Fig. 14, considering the large

difference of transmission loss between the 250 and 300 kg/m^3 groups. Moreover, even within the density groups, the transmission loss was closely correlated to the density of the boards. As presented in Fig. 6, the density of all the 250 kg/m^3 boards was very similar, in the order of 250 > 250-5 > 250-10. Likewise, the transmission losses of these boards were very close, and they followed the same order. For the 300 kg/m^3 boards, the difference in density was quite important and in the order of 300-10 > 300-5 > 300. Again, the difference of transmission loss of these boards is quite important and follow the same order.

Table 8. Average Normal Incident Transmission Loss and Absorption Coefficient of the Boards, Between 117 and 4322 Hz

Boards	Transmission Loss (Db)	Absorption Coefficient
250	23.28	0.51
250-5	21.85	0.49
250-10	19.52	0.59
300	31.96	0.32
300-5	37.51	0.33
300-10	41.38	0.22

In contrast, a lower density favors a better absorption coefficient. This is also evident from Table 8, where the 250 kg/m^3 boards possessed an average absorption coefficient almost twice as high as that of the 300 kg/m^3 ones. This table efficiently portraits the duality between the transmission loss and the absorption coefficient, as the very light 250-10 boards exhibited a quite low transmission loss (19.52 Db) and a high absorption coefficient (0.59), while the very dense 300-10 boards displayed a high transmission loss (41.38 Db) and a low absorption coefficient (0.22).

Regarding the density, the corn starch content seems to have had a negligible effect on the acoustic properties of the presented boards.

In contrast to hemp-lime where peaks in sound absorption are seen at 600 Hz and 1800 Hz with a marked trough at 1100 Hz (Degrave-Lemeurs *et al*. 2018), this material showed noticeably less fall-off in this range, probably due to the nature of the binder.

DISCUSSION

The kinetics of the reaction were somewhat slower than those commonly seen in the manufacture of particle boards using formaldehyde-based thermosetting adhesives. In addition, the reaction temperature of 160 °C is considerably higher than temperatures required for formaldehyde-based thermosetting adhesives, which can be as low as 110 °C. These issues mean that it is not possible to directly substitute the glycerol-based adhesive into existing production lines without increasing temperatures and slowing down production rates to an uneconomical extent. It is postulated that the use of microwaves or radio-frequency as part of the production line could achieve the required cross-linking temperatures more rapidly thereby reducing the time needed to achieve polymerization to match the production rates currently seen in the industry.

In addition, further work is required to reduce the sensitivity of the board to moisture. This is likely to be achieved through the inclusion of hydrophobic additives into the binder, such as silanes or paraffin wax, which would be compatible with the binder's chemistry. More work is required to achieve this goal.

Benefits of achieving this would include:

1. Elimination of VOC emissions due to elimination of formaldehyde
2. Lower environmental impact due to the use of a bio-based by-product from the bio-diesel industry
3. Lower environmental impact due to the use of short-cycle crops in place to timber-based particles.
4. Creation of a new class of low density particle board with low thermal conductivity and excellent acoustic properties

CONCLUSIONS

1. This study demonstrated that it was possible to make a particle board using hemp shiv as an aggregate with a thermo-setting binder made from crude glycerol and citric acid.
2. The particle board created had a significantly lower density than the current range of particle boards at 250 kg/m^3 compared with 600 to 700 kg/m^3 for boards currently available in the market.
3. The particle board had a significantly lower thermal conductivity than the current range of particle boards at 0.07 W/m.K compared with 0.13 W/m.K for boards currently available in the market.
4. The particle board had a significantly greater vapour permeability than the current range of particle boards at 10 to 15 μ compared with 100 to 450 μ for boards currently available in the market
5. The particle board had a broader spectrum of sound absorption, particularly at lower frequencies than the current range of particle boards.
6. The boards that have been produced exhibited the potential to be used as sound insulation boards on the interior of buildings, with the added benefit of also being thermally insulating. Because they are fabricated using an industrial waste-stream they would have an additional selling point of having a lower environmental impact than competitive products.

ACKNOWLEDGMENTS

The authors are grateful for the support of Innovate UK award no 10067643.

REFERENCES CITED

Ahmad, M. R., Chen, B., Oderji, S. Y., and Mohsan, M. (2018). "Development of a new bio-composite for building insulation and structural purpose using corn stalk and magnesium phosphate cement," *Energy and Building* 173, 719-733. DOI: 10.1016/j.enbuild.2018.06.007

Albaalbaki, B., and Hill, R. J. (2012). "On the molecular diffusion in nanostructured porous media: Interfacial exchange kinetics and surface diffusion," *Proc. R. Soc. A* 468, 3100-3120. DOI: 10.1098/rspa.2012.0172

Albrecht, K., Neudecker, F., Veigel, S., Bodner, S., Keckes,J., and Gindl-Altmutter, W. (2023). "The suitability of common reed (Phragmites australis) for load-bearing structural materials," *Journal of Materials Science* 58, 15411-15420. DOI: 10.1007/s10853-023-08996-1

Amziane, S., Collet, F., Lawrence, M., Magniont, C., Picandet, V., and Sonebi, M. (2017). "Recommendation of the RILEM TC 236-BBM: Characterisation testing of hemp shiv to determine the initial water content, water absorption, dry density, particle size distribution and thermal conductivity," *Materials and Structures* 50, 167. DOI: 10.1617/s11527-017-1029-3

ASTM C518-21 (2021). "Standard test method for steady-state thermal transmission properties by means of the heat flow meter apparatus," ASTM International, West Conshohocken, PA.

ASTM D1037-12 (2020). "Evaluating properties of wood-base fiber and particle panel materials," ASTM International, West Conshohocken, PA.

ASTM E96-22a (2022). "Gravimetric determination of water vapor transmission rate of materials," ASTM International, West Conshohocken, PA.

ASTM E2611-19 (2019). "Standard test method for normal incidence determination of porous material acoustical properties based on the transfer matrix method," ASTM International, West Conshohocken, PA.

Barbhuiya, S., and Das, B. (2022). "A comprehensive review on the use of hemp in concrete," *Construction and Building Materials* 341. DOI: 10.1016/j.conbuildmat.2022.127857

Berube, M-A., Schorr, D., Ball, R., Landry, V., and Blanchet, P. (2018). "Determination of *in situ* esterification parameters of citric acid-glycerol based polymers for wood impregnation," *J.Polym Environ*. DOI: 10.1007/s10924-017-1011-8

Biancaniello, M., Wang, T., Misra, M., and Mohanty, A. K. (2017). "Plywood adhesives derived from distillers' dried grains with solubles (DDGS) incorporating 2-hydroxyethyl acrylate," *Journal of Applied Polymer Science* 135(6), article 45689. DOI: 10.1002/app.45689

Chen, S., Aladejana, J. T., Li, X., Bai, M., Shi, S. Q., Kang, H., Cao, J., and Li, J. (2023). "A strong, antimildew, and fully bio-based adhesive fabricated by soybean meal and dialdehyde chitosan," *Industrial Crops and Products* 194, article 116277. DOI: 10.1016/j.indcrop.2023.116277

Cowan, J. (2014). "Building acoustics," in: *Springer Handbook of Acoustics*, T. D. Rossing (ed.), Springer Handbooks, Springer, New York, NY. DOI: 10.1007/978-1-4939-0755-7_11

Degrave-Lemeurs, M., Glé, P., and Hellouin de Menibus, A. (2018). "Acoustical properties of hemp concretes for buildings thermal insulation: Application to clay and lime binders," *Construction and Building Materials* 160, 462-474. DOI: 10.1016/j.conbuildmat.2017.11.064

Diaz Fuentes, C. X., Pérez Rojas, M. C., and Mancilla J. J. (2020). "Physical-thermal straw properties advantages in the design of a sustainable panel-type construction system to be used as an architectural dividing element," *Journal of Physics* 1587, article 012032. DOI: 10.1088/1742-6596/1587/1/012032

Dunky, M. (2003). "Adhesives in the wood industry," in: *Handbook of Adhesive Technology* (2nd Ed.), A. Pizzi and K. L. Mittal (eds.), Marcel Dekker Inc, New York.

EN ISO 12572 (2016). "Hygrothermal performance of building materials and products – Determination of water vapour transmission properties – cup method (ISO

12572:2016)," European Committee for Standardisation, Brussels, Belgium.
Essoua Essoua, G., Blanchet, P., Landry, V., and Beauregard, R. (2016). "Pinewood treated with a citric acid and glycerol mixture: Biomaterial performance improved by a bio-byproduct," *BioResources* 11(2), 3049-3072. DOI: 10.15376/biores.11.2.3049-3072
European Commission (2023). "Hemp," (https://agriculture.ec.europa.eu/farming/crop-productions-and-plant-based-products/hemp_en).
Hemmilä, V., Adamopoulos S., Karlsson, O., and Kumar, A. (2017). "Development of sustainable bio-adhesives for engineered wood panels— A review," *RSC Advances* 7, 38604-38630.
Holser, R. (2008). "Thermal analysis of glycerol citrate/starch blends," *Journal of Applied Polymer Science*. DOI: 10.1002/app.27651
Hu, S., Luo, X., Wan, C., and Li, Y. (2012). "Characterization of crude glycerol from biodiesel plants," *J. Agric. Food Chem.* 60(23), 5915-5921. DOI: 10. 1021/ jf300 8629
Hussain, A., Calabria-Holley, J., Lawrence, M., Ansell, M., Jiang, Y., Schorr, D., and Blanchet, P. (2019). "Development of novel building composites based on hemp and multi-functional silica matrix," *Composited Part B* 156, article 2660273. DOI: 10.1016/j.compositesb.2018.08.093
IsoHemp SA (2024). IsoHemp data sheet, Fernelmont, Belgium.
Kan, A., Zhang, X., Chen, Z., and Cao, D. (2023). "Effective thermal conductivity of vacuum insulation panels prepared with recyclable fibrous cotton core," *International Journal of Thermal Sciences* 187, article 108176. DOI: 10.1016/j.ijthermalsci.2023.108176
Kulshreshtha, Y., Schlangen, E., Jonkers, H. M., Vardon, P. J., and van Paassen, L. A. (2017). "CoRncrete: A corn starch based building material," *Construction and Building Materials* 154, 411-423. DOI: 10.1016/j.conbuildmat.2017.07.184
Latif, E., Lawrence, M., Shea, A., and Walker, P. (2015). "Moisture buffer potential of experimental wall assemblies incorporating formulated hemp-lime," *Building and Environment* 93(2), 199-209. DOI: 10.1016/j.buildenv.2015.07.011
Lawrence, M. (2015). "Reducing the environmental impact of construction by using renewable materials," *J. Renew. Mater.* 3, 163-174. DOI: 10.7569/JRM.2015.634105
Li, C., Hou, D., Xi., X., Lei, H., Tondi, G., Shi, J., and Du, G. (2024). "Eco-friendly biobased adhesives prepared from different polyester-type glucose with high cross-linked structure," *ACS Sustainable Chemistry & Engineering* 12(20), 7831-7843. DOI: 10.1021/acssuschemeng.4c00669
Liu, L., Jia, Y., Zheng, L., Luo, R., Essawy, H., Huang, H., Wang, Y., Deng, S., and Zhang, J. (2024). "Development and characterization of bio-based formaldehyde free sucrose-based adhesive for fabrication of plywood," *Polymers* 16(5), article 640. DOI: 10.3390/polym16050640
Mary, A., Blanchet, P., Pepin, S., Chamberland, J., and Landry, V. (2024a). "Upcycling of protein concentrates from industrial byproducts into polyurethane wood adhesives," *BioResources* 19(1), 1165-1189. DOI: 10.15376/biores.19.1.1165-1189
Mary, A., Blanchet, P., Pepin, S., Hermann, A., Charron, S., and Landry, V. (2024b). "Industrial byproducts as adhesive allies: Unraveling the role of proteins and isocyanates in polyurethane wood bonding," *BioResources* 19(2), 3520-3542. DOI: 10.15376/biores.19.2.3520-3542
Mucsi, Z. M., Faridul Hasan, K. M., Horvath, P. G., Bak, M., Koczan, Z., and Alpar, T.

(2022). "Semi-dry technology mediated lignocellulosic coconut and energy reed straw reinforced cementitious insulation panels," *Journal of Building Engineering* 57, article 104825. DOI: 10.1016/j.jobe.2022.104825

Nguyen, D. T. and Pham, Q. T. (2020). "A theoretical and experimental study on esterification of citric acid with the primary alcohols and the hydroxyl groups of cellulose chain (n = 1-2) in parched condition," *Journal of Chemistry*, Article no. 8825456. DOI: 10.1155/2020/8825456

Nitu, I., Rahman, S., Islam, M., Ashaduzzaman, M., and Shams, M. (2022). "Preparation and properties of jute stick particleboard using citric acid-glycerol mixture as a natural binder," *Journal of Wood Science*. DOI: 10.1186/s10086-022-02039-0

Osvaldova, L. M., Markova, I., Jochim, S., and Bares, J. (2021). "Experimental study of straw-based eco-panel using a small ignition initiator," *Polymers* 13(8), article 1344. DOI: 10.3390/polym13081344

Quintana-Gallardo, A., Clausell, J. R., Guillén-Guillamon, I., and Mendiguchia, F. A. (2021). "Waste valorization of rice straw as a building material in Valencia and its implications for local and global ecosystems," *Journal of Cleaner Production* 318, article 128507. DOI: 10.1016/j.jclepro.2021.128507

Rode, C., and Grau, K. (2008). "Moisture buffering and its consequence in whole building hygrothermal modeling," *Journal of Building Physics* 31(4), 333-360. DOI: 10.1177/1744259108088960

Royal Academy of Engineering (2021). "Decarbonising construction: Building a new net zero industry," (https://nepc.raeng.org.uk/policy-work/net-zero/decarbonising-construction), Accessed 10 July 2024.

Salthammer, T., Mentese, S., and Marutzky, R. (2010). "Formaldehyde in the indoor environment," *Chem. Rev.* 110(4), 2536-2572. DOI: 10.1021/cr800399g

Savas, S., Bakir, D., and Akcaat, Y. K. (2024). "Experimental and numerical investigation of the usability of nonwoven hemp as a reinforcement material," *Case Studies in Construction Materials* 20, article e03091. DOI: 10.1016/j.cscm.2024.e03091

Segovia, F., Blanchet, P., Auclair, N., and Essoua Essoua, G. G. (2020). "Thermo-mechanical properties of a wood fiber insulation board using a bio-based adhesive as a binder," *Buildings* 10(9), article 152. DOI: 10.3390/buildings10090152

Segovia, F., Blanchet, P., and Essoua Essoua, G. (2021). "Potential of the crude glycerol and citric acid mixture as a binder in medium-density fiberboard manufacturing," *European Journal of Wood and Wood Products*. DOI: 10.1007/s00107-021-01719-w

Soccol, C. R., Vandenberghe, L. P. S., Rodriques, C., and Pandey, A. (2006). "New perspectives for citric acid production and application," *Food Technol. Biotechnol.* 44, 141. DOI: 10.17113/ftb-1643

Silva, A., Gaspar, F., and Bakatovich, A. (2023). "Composite materials of rice husk and reed fibers for thermal insulation plates using sodium silicate as a binder," *Sustainability* 15(14), article 11273. DOI: 10.3390/su151411273

Smartply (2024). "Ultima data sheet," (www.mdfosb.com), accessed 14 March 2024.

Tisserat, B., O'kuro, R., Hwang, H., Mohamed, A., and Holser, R. (2012). "Glycerol citrate polyesters produced through heating without catalysis," *Journal of Applied Polymer Science* 125, 3429-3437. DOI: 10.1002/app.36669

Tlaiji, G., Ouldboukhitine, S., Pennec, F., and Biwole, P. (2022). "Thermal and mechanical behavior of straw-based construction: A review," *Construction and Building Materials* 316, article 125915. DOI: 10.1016/j.conbuildmat.2021.125915

Wankhede, B., Bisaria, H., and Dakre, V. S. (2022). "A review on cotton fibre-reinforced polymer composites and their applications," *Journal of Materials: Design and Applications* 237(6), 1347-1362. DOI: 10.1177/1464420722114387

World Green Building Council (2022). "Advancing net zero status report," (www.worldgbc.org/reports), Accessed 10 July 2024.

Xi, X., Pizzi, A., Gerardin, C., Liao, J., Amirou, S., and Abdalla, S. (2019). "Glutaraldehyde-wheat gluten protein adhesives for wood bonding," *The Journal of Adhesion* 97(1), 88-100. DOI: 10.1080/00218464.2019.1630821

Yang, H., Wu, Y., Ni, K., Liu, T., Ran, X., Tan, X., Gao, W., Yang, Z., Du, G., and Yang, L. (2023). "Integration of branched amine and dialdehyde cellulose to produce high-performance bio-based wood adhesive," *International Journal of Adhesion and Adhesives* 126, article 103449. DOI: 10.1016/j.ijadhadh.2023.103449

Yuan, J., Du, G., Yand, H., Liu, S., Park, S., Liu, T., Ran, X., Park, B-D., Gao, W., and Yang, L. (2023). "Fully bio-based adhesive designed through lignin-cellulose combination and interfacial bonding reinforcement," *Industrial Crops and Products* 204(A), article 117279. DOI: 10.1016/j.indcrop.2023.117279

Zhao, Z., Zhang, W., Cai, W., Sun, S., and Yong, Q. (2023). "Preparation and investigation of a fully biobased adhesive composed of gum arabic and soy protein isolate for plywood," *ACS Sustainable Chemistry & Engineering* 11(44), 16005-16014. DOI: 10.1021/acssuschemeng.3c05313

Article submitted: July 8, 2024; Peer review completed: July 17, 2024; Revised version received: July 31, 2024; Accepted: August 14, 2024; Published: October 21, 2024.
DOI: 10.15376/biores.19.4.9310-9333